JOURNAL OF GEOPHYSICAL RESEARCH, VOL. 112, D11210, doi:10.1029/2006JD007698, 2007

Source evaluation of aerosols measured during the Indian Ocean Experiment using combined chemical transport and back trajectory modeling

S. Verma,[1] C. Venkataraman,[1] O. Boucher,[2,3] and S. Ramachandran[4]

Received 25 June 2006; revised 19 February 2007; accepted 22 March 2007; published 9 June 2007.

[1] This work presents an analysis of aerosol measurements made during the Oceanographic Research Vessel *Sagar Kanya* cruise of January–March 1999, in the Indian Ocean Experiment intensive field phase (INDOEX-IFP), with regard to the aerosol chemical constituents and identification of source regions of their origin. This is done through a hybrid approach which uses an Eulerian forward transport calculation in a general circulation model (GCM) with region-tagged emissions along with an analysis of Lagrangian back trajectories and emission inventory information, for overlapping time periods. Back trajectory analysis showed that the ship was mainly influenced by air masses from the Indo-Gangetic plain, central India, or south India during the early part of its cruise with the GCM-predicted aerosol species composed of mainly sulfate and organic matter, whereas dust species dominated during its cruise in late February and early March over the Arabian Sea when the ship was influenced by air masses from Africa-west Asia or northwest India. However, a typical clean marine aerosol dominated by sea salt was encountered during February when the ship cruised in the tropical Indian Ocean and was mostly influenced by marine air masses. The high aerosol optical depth was due to roughly equal parts of organic matter and sulfate. Region-tagged GCM estimates showed the presence of distinct transport at surface and higher layers for, e.g., DOY 56–61 and 65–70, indicating strong signals of emissions of black carbon, organic matter, and sulfate originating in central and northwest India, whereas elevated transport channels of black carbon and organic matter from Africa-west Asia. This is consistent with the back trajectory analysis and in corroboration with INDOEX measurement studies which observed different aerosol properties from aircraft and ship attributed to different transport pathways in surface and elevated flows. However, back trajectory analysis is not sufficient to evaluate the major source regions contributing to the transported aerosol. The fractional contribution of a source region also depended upon the emission flux from the region and its proximity to the receptor domain.

Citation: Verma, S., C. Venkataraman, O. Boucher, and S. Ramachandran (2007), Source evaluation of aerosols measured during the Indian Ocean Experiment using combined chemical transport and back trajectory modeling, *J. Geophys. Res.*, *112*, D11210, doi:10.1029/2006JD007698.

1. Introduction

[2] Observational studies during the Indian Ocean Experiment or INDOEX [*Ramanathan et al.*, 2001; *Ramachandran and Jayaraman*, 2002] and more recent field campaigns in the Bay of Bengal [*Ramachandran*, 2005; *Lal et al.*, 2006] Arabian Sea [*Rao*, 2005] have established the widespread occurrence of aerosols and trace gases of anthropogenic origin over ocean regions adjoining India. Several INDOEX investigators analyzed transport pathways into the domain and variations in pollution loading in air masses of different origins. Four broad channels of flow were identified into the INDOEX domain during the winter monsoon [*Verver et al.*, 2001], which arose from west Asia passing over northwestern India, the Indo-Gangetic plain passing over the Bay of Bengal and south India, central India passing over the west coast and from southeast Asia, indicating contributions of multiple regions to the measured pollutants. Back trajectory analysis was used to qualitatively link variations in the chemical and optical properties of aerosols [*Reiner et al.*, 2001; *Mayol-Bracero et al.*, 2002; *Quinn et al.*, 2002; *Franke et al.*, 2003] to sources, broadly biomass burning and fossil fuel combustion, located in geographical regions traversed by

[1]Department of Chemical Engineering, Indian Institute of Technology, Bombay, Mumbai, India.
[2]Laboratoire d'Optique Atmosphérique, CNRS/Université des Sciences et Technologies de Lille, Villeneuve d'Ascq, France.
[3]Now at Hadley Centre, Met Office, Exeter, UK.
[4]Space and Atmospheric Sciences Division, Physical Research Laboratory, Ahmedabad, India.

0148-0227/07/2006JD007698$09.00

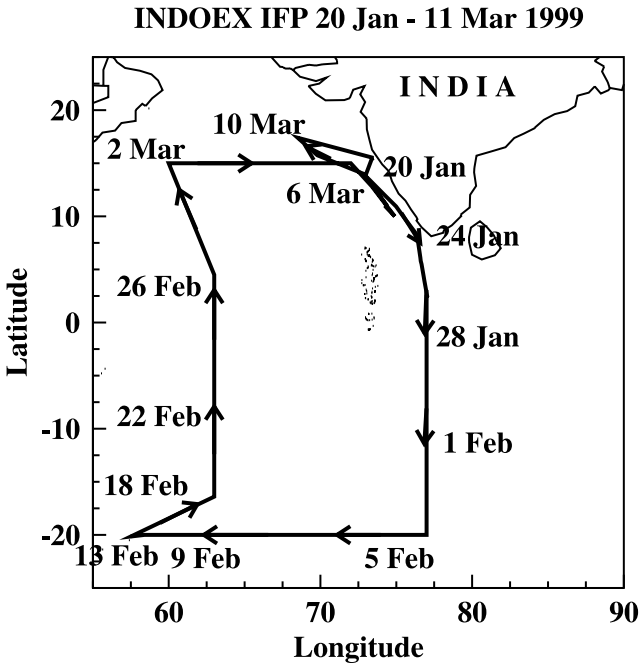

Figure 1. Map of the *Sagar Kanya* ship cruise during INDOEX-IFP with the ship position marked on the map on individual days.

air masses arriving in the Arabian Sea and tropical Indian Ocean. *Quinn et al.* [2002] suggested eight source regions, based on back trajectory pathways influencing the *Ronald H. Brown* ship during its INDOEX cruise. They identified periods when the boundary layer and elevated layer aerosols were well mixed, and contrasting periods when they were not well mixed, in both cases arising from the same or different source regions. In situ chemical measurements showed the presence of high sulfate, particulate organic matter, black carbon, and inorganic matter in the air masses from Arabia and the Indian subcontinent than in marine air masses. Aircraft based measurements of trace gas concentrations, aerosol chemical composition and optical effects over the Indian Ocean during INDOEX showed the evidence of the signatures of heavy pollution over the north Indian ocean which was identified because of the outflow from the Indian subcontinent as well as from Arabia and Southeast Asia based on back trajectory calculations [*Reiner et al.*, 2001; *de Gouw et al.*, 2001; *Gabriel et al.*, 2002; *Mayol-Bracero et al.*, 2002]. *Leon et al.* [2001] suggested the episodic transport of dust from Arabia over the Indian Ocean region during INDOEX.

[3] Modeling methods for source-receptor resolution, or quantitative estimation of the contribution of various sources, source classes or source regions to measured atmospheric pollution, e.g., mass concentrations of aerosol particles, aerosol chemical constituents or gaseous pollutants, are broadly classified as dispersion models and receptor models. Dispersion models use mathematical descriptions of sources, in the form of emission inventories, and of atmospheric processes including dilution, chemical transformation and transport to predict pollutant concentrations over space and time, and form the basis of chemical transport models [*Seinfeld and Pandis*, 1998]. Retrotransport and adjoint modeling [*Hourdin and Issartel*, 2000] are used to estimate source region contributions by running chemical transport models backward in time. Receptor models use pollutant characteristics, such as chemical composition and their time series variation, at the receptor site, along with source information, to identify sources and their quantitative contributions to the measured pollution at the receptor site [*Friedlander*, 1973; *Hopke*, 2003]. Receptor modeling methods using back trajectories that arise from a receptor site to identify contributing source regions, include residence time and area of influence analysis and the potential source contribution function [*Hopke*, 2003]. Hybrid models, e.g., trajectory cluster analysis with chemical mass balance receptor modeling [*Woo et al.*, 2003] and factor analysis or positive matrix factorization with back trajectory analysis [*Kulkarni et al.*, 2005] are recently being tried for regional-scale source-receptor resolution. Additionally, inverse modeling [*Kasibhatla and Arellano*, 2002] uses optimization methods to vary regional source strengths and minimize errors between global measurement databases and predictions from chemical transport models run in forward time, to deduce potential errors in emission inventories.

[4] Dispersion models, i.e., chemical transport models, have been used with newly available regional emissions information for atmospheric simulations over south Asia during the INDOEX period [*Reddy et al.*, 2004; *Verma et al.*, 2006], and have shown a predominance of organic carbon aerosols in addition to sulfate in the south Asian region. Modeling studies have indicated the potential contribution of regions outside India to INDOEX aerosols [*Rasch et al.*, 2001; *Reddy et al.*, 2004], and of biomass burning to carbon monoxide [*de Laat et al.*, 2001; *Lelieveld et al.*, 2001]. A mesoscale chemical transport model has been used to analyze sulfate, carbonaceous and dust transport indicated the predominance of dust species over the North while that of sulfate and carbonaceous species in the south of the INDOEX area [*Minvielle et al.*, 2004a, 2004b]. In this work, we analyze the aerosol species composition to the aerosol distributions measured on board the Oceanographic Research Vessel *Sagar Kanya* during its INDOEX-IFP cruise. We carry out the source identification of the transported aerosol using a hybrid method which involves region-tagged emissions in an Eulerian forward transport calculation in a general circulation model (GCM) along with analysis of Lagrangian back trajectories and emission inventory information, for overlapping time periods.

2. Method of Study

[5] The analysis carried out refers to the ship cruise expedition of Oceanographic Research Vessel *Sagar Kanya* (cruise 141) for the period from 20 January (DOY 20) to 12 March (DOY 71) 1999 covering a domain from 20°S to 17.2°N and 57.5°E to 77°E [*Ramachandran and Jayaraman*, 2002]. Figure 1 shows the map of *Sagar Kanya* cruise during INDOEX-IFP with the ship position marked on the map on individual days. In order to assess the influence of various source regions on the spatial distributions of aerosols measured during the cruise, the following method is used in this work: (1) In the absence of simultaneous aerosol chemical measurements for the ship cruise, aerosol chemical species composition is predicted through aerosol transport simulations in the general circulation model of the Laboratoire de Météorologie Dynamique (LMD-ZT GCM) for INDOEX

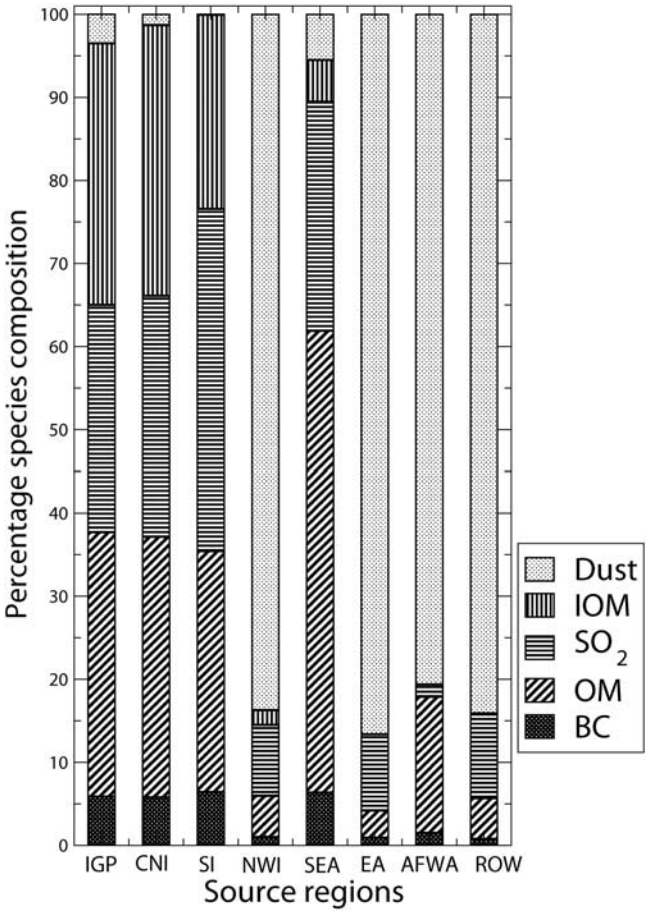

Figure 2. Regional emission composition of classified source regions of IGP, CNI, SI, NWI, SEA, EA, AFWA, and ROW based on emission of species from inventories implemented in LMD-ZT GCM. The total emission flux averaged over the source regions for the given aerosol species in Tg yr^{-1} are as follows: IGP (4.88), CNI (3.25), SI (0.83), NWI (4.7), SEA (3.02), EA (112), AFWA (566), and ROW (462).

and sampling the estimates for the times and locations of *Sagar Kanya* during its INDOEX-IFP cruise. (2) We use source region aerosol flux composition, from the emission inventory to deduce their potential influence on receptor location. (3) We make quantitative predictions of source region contributions to total aerosols and aerosol chemical species, through aerosol transport experiments in the LMD-ZT GCM with region-tagged emissions in conjunction with the back trajectory analysis.

2.1. Aerosol Emission Fluxes From Source Regions

[6] Source regions were classified on the basis of differences in composition of their aerosol emission fluxes and their proximity to the Indian Ocean [*Rasch et al.*, 2001; *Ramachandran and Jayaraman*, 2002; *Reddy et al.*, 2004]. These source regions are the following: (1) Indo-Gangetic plain (IGP), (2) central India (CNI), (3) south India (SI), (4) northwest India (NWI), (5) southeast Asia (SEA), (6) east Asia (EA), (7) Africa-west Asia (AFWA), and (8) rest of the world (ROW). Emissions over India are from the high-resolution ($0.25° \times 0.25°$) emission inventories of *Reddy and Venkataraman* [2002a, 2002b]. Emissions of SO_2, BC, and organic carbon (OC) from fossil fuel and biomass sources over Asia are from *Streets et al.* [2003]. Global aerosol emissions used here are the same as described by *Reddy and Boucher* [2004] and *Reddy et al.* [2004]. Emission fluxes were aggregated spatially over each source region for the aerosol species including BC, OM, sulfur dioxide (SO_2), inorganic matter (IOM) and dust. Figure 2 shows the percentage composition of regional emissions for the source regions. The total emission flux averaged over the source regions for the given aerosol species are indicated in the caption of Figure 2. Out of the parts of Indian region (Indo-Gangetic plain, central India, south India, northwest India), Indo-Gangetic plain has the highest emission flux followed by that of northwest India, central India, and south India. Emission fluxes from the Indo-Gangetic plain, central India, south India are mainly composed of sulfate, organic matter, inorganic matter followed by black carbon. Northwest India emissions are mainly dust followed by sulfate. Southeast Asia emissions are mainly composed of organic matter followed by sulfate. Africa-west Asia emissions are mainly composed of dust and organic matter. Emission flux from east Asia and rest of the world are mainly composed of dust followed by sulfate. On looking at the emission map for the ratio of fossil fuel to biomass burning sources for India and the identified dominant sources of aerosols in Indian region [*Habib et al.*, 2006], it is seen that Indo-Gangetic plain, central India are dominated by both the fossil fuel and biomass burning sources with the predominant contributions from fossil fuel sources over south India and northwest India. The characteristic emission composition of regions can be used to deduce their potential influence on receptor location or domain.

2.2. Back Trajectory Calculations

[7] Transport from source region to receptor locations can be qualitatively assessed from a knowledge of pathways of air mass movement between sources and receptor. Back trajectories offer a method of tracking the path of an air parcel. The back trajectories are calculated with the help of NOAA HYSPLIT (Hybrid Single-Particle Lagrangian Integrated Trajectory) (Version 4) model [*Draxler and Hess*, 1998]. The velocity field and temperature fields used to calculate the trajectories are taken from NCEP data archives (ftp://www.arl.noaa.gov/pub/archives/fnl). Back trajectories integrate back in time to track the path of travel of an air parcel arriving at a receptor location at a given time. However, back trajectories do not take into account mixing between air masses at various heights. A simple grouping of various trajectory pathways can provide a more realistic representation of plume dispersion to categorize the source region. All the back trajectories were calculated at 1200 h Indian Standard Time (+0530 h GMT). As the residence time of aerosols is of the order of a week in the lower atmosphere, 7-days back trajectory analyzes were performed. The 7-days back trajectories were calculated for the days and positions of *Sagar Kanya* during its INDOEX-IFP cruise from 20 January (DOY 20) to 11 March (DOY 70), 1999 at five heights (10 m, 100 m, 500 m, 1000 m, 5000 m). This corresponded to 250 back trajectory data sets. Most of the trajectories at surface level

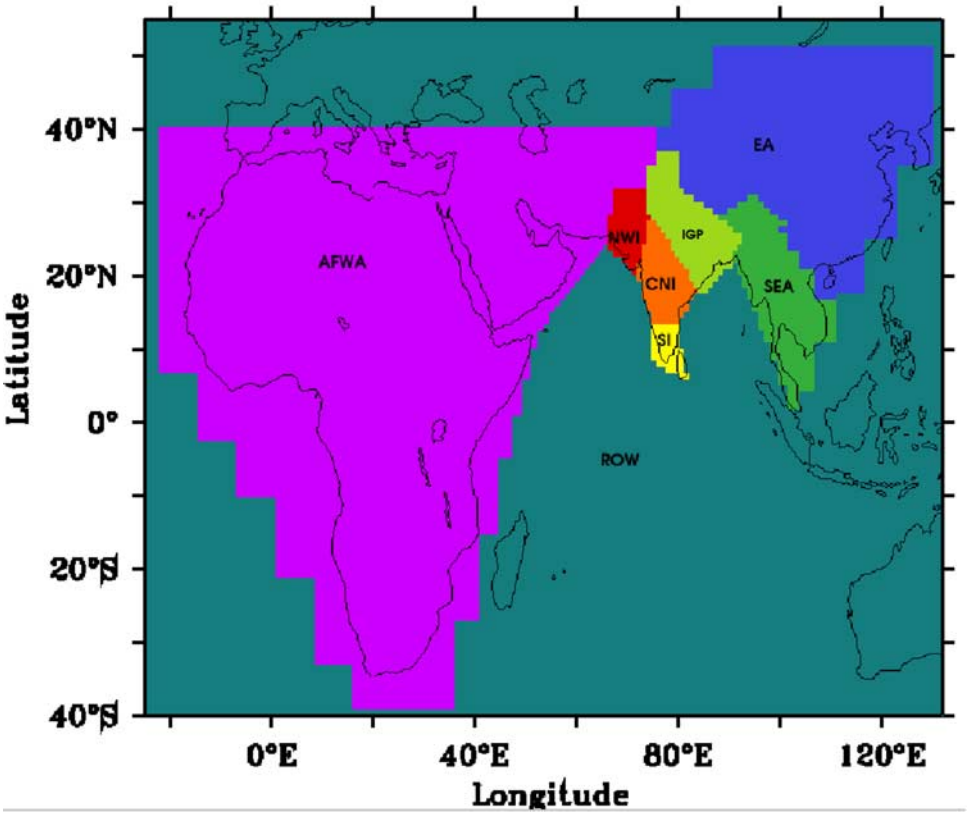

Figure 3. Masked regions on GCM zoom grid representing tagged source regions taken under study; the classification of source regions are as follows with different color scales indicated in bracket: (1) IGP (light green), (2) CNI (orange), (3) SI (yellow), (4) NWI (red), (5) SEA (green), (6) EA (blue), (7) AFWA (purple), and (8) ROW (dark green).

(10 m to 500 m) originate from the Indian region and that at higher heights (1000 m and above) from Africa-west Asia and the Indo-Gangetic plain indicating the presence of long-range transport from Africa-west Asia over to the Indo-Gangetic plain.

2.3. Short Description of the LMD-ZT GCM

[8] The study of region-tagged aerosol transport is carried out with the help of the LMD-ZT general circulation model (GCM), version 3.3. A description of the atmospheric model is given by *Li* [1999] and a specific description of aerosol treatment and atmospheric transport is given by *Boucher et al.* [2002] and *Reddy et al.* [2004]. A short description of the model is presented here. The sulfur cycle has been incorporated and processes of convective transport, wet scavenging, and aqueous phase chemistry have been parameterized as consistently as possible with the model physical parameterizations [*Boucher et al.*, 2002]. Sulfate formation, transport, and radiative forcing were estimated by *Boucher et al.* [2002]. Aerosol optical properties (mass extinction coefficient, α_e; single scattering albedo, ω; and asymmetry factor, g) for all aerosol species are computed using Mie theory as described by *Reddy et al.* [2004]. The aerosol extinction coefficient is computed from all aerosol species and associated water.

[9] The model has a resolution of 96 points in longitude and 72 points in latitude. There are 19 vertical layers of a hybrid sigma-pressure coordinate with eleven layers below 850 hPa and eight layers between 850 and 500 hPa. A zoom is applied over the Indian region; it is centered at 75°E and 15°N and extends from 50°E to 100°E in longitude and from 5°S to 35°N in latitude. Zoom factors of 4 and 3 are applied in longitude and latitude, respectively, resulting in a resolution of about 1° in longitude and 0.8° in latitude over the zoomed region. A short description of the technique applied to use the GCM with tagged region as an Eulerian forward transport approach is given here. The source regions as classified in section 2.1 are implemented in GCM. Figure 3 shows the masked regions on GCM zoom grid. Aerosol emissions including sulfate (Sul), organic matter (OM), black carbon (BC), dust, inorganic matter (IOM), and sea salt (SS) are tagged for each of the source region. INDOEX-IFP is simulated in the LMD-ZT GCM for each of the source region with the emissions out of that region being switched off. The GCM is nudged with ECMWF wind fields. We sample the model outputs for the different position and time of the *Sagar Kanya* during its INDOEX-IFP cruise.

3. Source Region Influence and Contribution to Aerosols Measured Aboard *Sagar Kanya*

3.1. Back Trajectory Analysis and Emission Inventory Information

[10] Back trajectories were calculated as described in section 2.2 and grouped on the basis of their origin and

Table 1. Sampling Days According to Back Trajectory Passing Through Different Identified Source Regions at 10, 100, 500, 1000, and 5000 m Heights for the Days of Year (DOY) of the Ship Cruise Expedition of *Sagar Kanya* During INDOEX-IFP[a]

	Sampled Days of Year (DOY)		
Source Region Groups	10–500 m	1000 m	5000 m
IGP/CNI/SI	CI: 20–25	CI: 20–21	CI: 22–23, 66
IGP/CNI/SI	AS: 26	AS: 26,63[b]	AS: nil
IGP/CNI/SI	TIO: 27–28	TIO: 28, 55[b]	TIO: nil
CNI/NWI	CI: 65–66	CI: 65–66, 67[b]	CI: nil
CNI/NWI	AS: 63–64	AS: 59[b], 60[b], 64	AS: 64
CNI/NWI	TIO: 55	TIO: nil	TIO: nil
AFWA/NWI	CI: 67–68	CI: 68	CI: 20–21[b]
AFWA/NWI	AS: 58, 59, 60–62, 69–70	AS: 61, 62, 69–70	AS: 59, 60–63
AFWA/NWI	TIO: nil	TIO: nil	TIO: nil
AFWA/IGP/CNI/SI	CI: nil	CI: 22–24,[b] 25[b]	CI: 65, 67[b]
AFWA/IGP/CNI/SI	AS: nil	AS: 58[b]	AS: nil
AFWA/IGP/CNI/SI	TIO: nil	TIO: 27[b]	TIO: nil
SEA	CI: nil	CI: nil	CI: 24,[b] 25[b]
SEA	AS: nil	AS: nil	AS: 26[b]
SEA	TIO: 57	TIO: 57	TIO: nil
ROW	CI: nil	CI: nil	CI: 68[b]
ROW	AS: nil	AS: nil	AS: 69–70[b]
ROW	TIO: 29–31, 32–54, 56	TIO: 29–31, 32–54, 56	TIO: 27, 28,[b] 29–31, 32–56, 57, 58[b]

[a]CI, days when the ship traversed over coastal India; AS, days when the ship traversed over Arabian Sea; TIO, days when the ship traversed over tropical Indian Ocean.
[b]DOY when trajectories at 1000 m and 5000 m heights passed through different regions than at 10 m to 500 m heights.

traverse over the eight source regions shown in the Figure 3. Source region groups were classified on the basis of both reported geographical origin of air masses by previous investigators [*Reiner et al.*, 2001; *Mayol-Bracero et al.*, 2002; *Quinn et al.*, 2002; *Franke et al.*, 2003] and back trajectory analysis for the days and locations of *Sagar Kanya* cruise. Emissions flux composition from emissions inventory information [*Reddy and Venkataraman*, 2002a, 2002b; *Streets et al.*, 2003] indicated eight regions with distinct emissions composition (Figure 2), as described in section 2.1. Analysis of the back trajectories revealed that they traversed more than one source region, e.g., Indo-Gangetic plain/central India/south India, potentially entraining different aerosol chemical species from the different regions. On this basis, six source region groups were identified (Table 1) which corresponded with the major pathways of air masses arriving over the Indian ocean region, which are consistent with the regions identified by INDOEX investigators in earlier work [*Quinn et al.*, 2002; *Ball et al.*, 2003]. The path of back trajectories over the source regions for the days sampled at heights of 10 m to 5000 m are represented in Figure 4. Air masses arising from the Indo-Gangetic plain, passing over central and south India (source region group 1, in Table 1) arrived at the sampling platform on board *Sagar Kanya*, primarily in the early part of the cruise, when the ship passed from coastal India (CI) to the Arabian Sea (AS) and the tropical Indian Ocean (TIO). In addition, these air masses once again reached the ship during the ship's return to coastal India in early March. On the basis of emission inventory information, the air masses would contain organic and black carbon aerosols, inorganic oxidized matter (fly-ash) and sulfate (see Figure 2). Air masses from northwest and central Indian (source region group 2) reached the ship largely toward the end of the cruise mostly in the Arabian Sea and coastal India regions. These air masses would contain significant mineral dust aerosols (Figure 2) in addition to carbonaceous and fly-ash aerosols and sulfate. Air masses came from Africa-west Asia (source region group 3 in Table 1) largely in late February and early March in the Arabian Sea region of the cruise. These air masses are likely to carry mineral dust, and also organic carbon and black carbon aerosols from open biomass burning activities in Africa. Elevated air masses from Africa-west Asia, passing over the Indo-Gangetic plain and central and south India (source region group 4) arrived at the ship in late January and once again in late February and early March. These would transport highly mixed aerosols from desert and biomass burning in Africa-west Asia (dust, BC, OM), and from biofuel and fossil fuel combustion and biomass burning (BC, OM, IOM, SO_4), in the Indian regions. Air masses from southeast Asia (source region group 5) arrived at the ship during late January (at higher heights) and late February (surface and elevated layers) and are likely to carry organic carbon aerosols with some black carbon and sulfate. Air masses from the rest of the world (source region group 6) arrived at the ship largely when it was in the tropical Indian Ocean both in late January and again in late February and early March, both at surface and elevated levels, likely to contain sulfate in addition to sea salt and dust.

3.2. Species Composition of the Ship Cruise Aerosol Measurements

[11] Model estimates are analyzed to evaluate the species composition to aerosol surface mass concentration and aerosol optical depth for the days of the ship cruise expedition of *Sagar Kanya* during INDOEX-IFP. Figure 5a shows the time series of aerosol mass concentration (sum of nucleation mode and accumulation mode) measured from QCM (Quartz Crystal Microbalance) on board *Sagar Kanya* during the INDOEX-IFP (20 January to 12 March 1999) with measurements corrected to 0% relative humidity (RH). These results are from *Ramachandran and Jayaraman* [2002] and based on classifying the oceanic region into

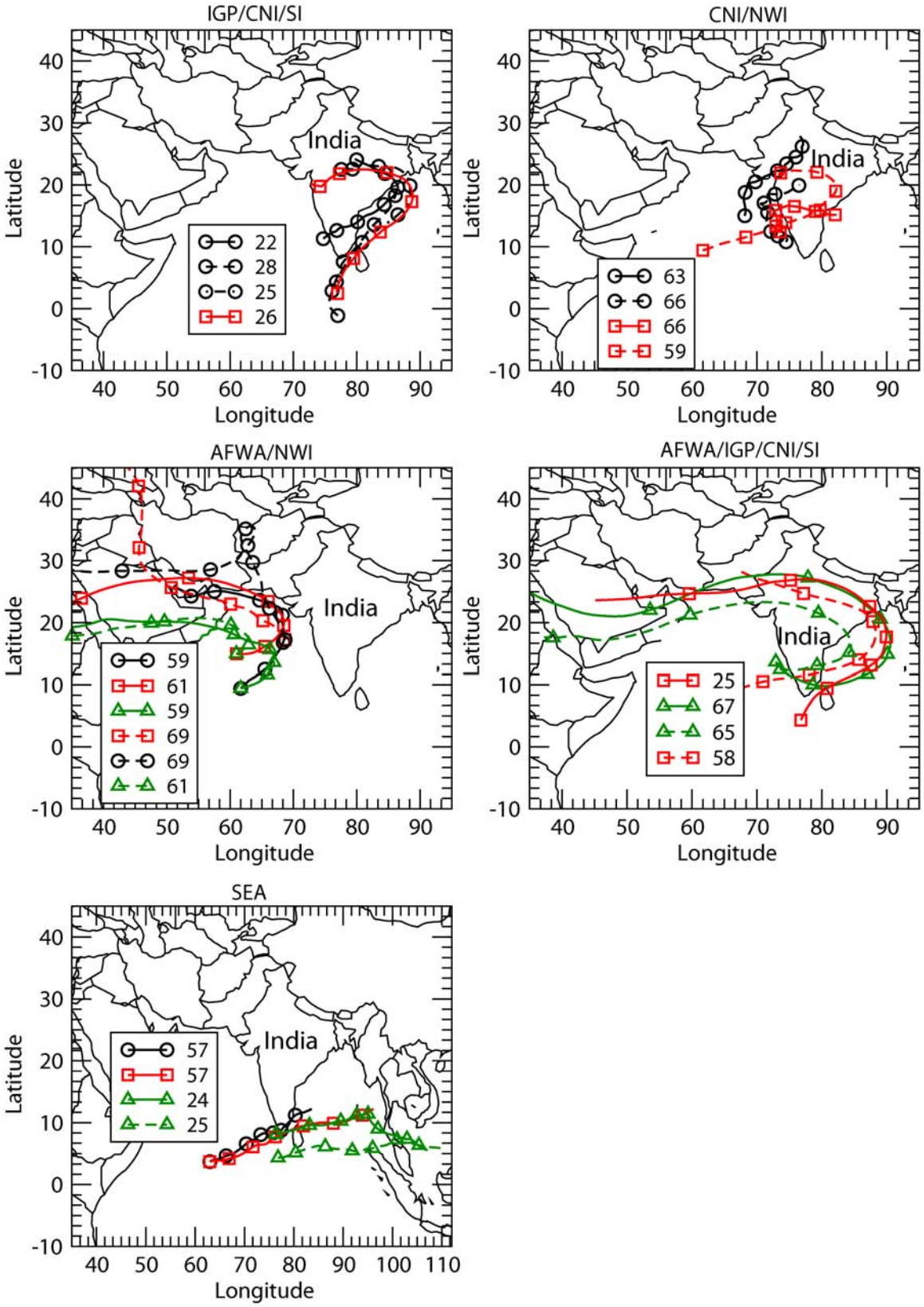

Figure 4. Path of back trajectories (10 m, 100 m, and 500 m (black lines with circles); 1000 m (red lines with squares); and 5000 m (green lines with triangles)) over the different identified source regions (details of back trajectories for all days of the ship cruise are given in Table 1). Numbers shown against the legends represent days of the year (DOY).

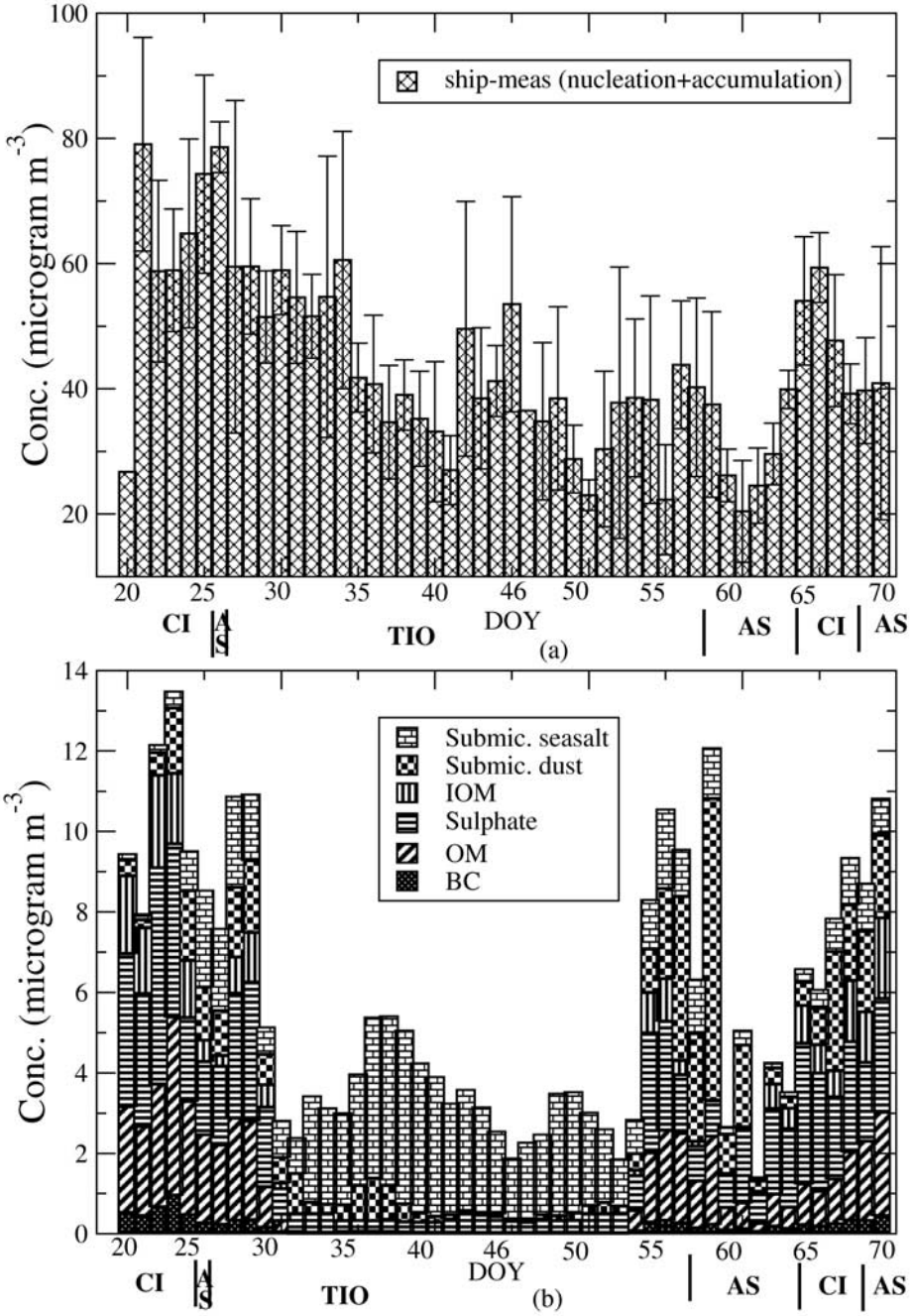

Figure 5. (a) Time series for the aerosol mass concentration (sum of nucleation and accumulation modes) measured at ambient RH and corrected for 0% RH from QCM on board *Sagar Kanya* during the INDOEX IFP and (b) species contribution to aerosol surface mass concentration from model estimates for the days of the ship cruise expedition of *Sagar Kanya* during INDOEX-IFP. DOY represents days of the year from 20 January to 11 March 1999. Traverse of the ship over the oceanic regions are represented by CI (coastal India), AS (Arabian Sea), and TIO (tropical Indian Ocean).

coastal India (CI), Arabian Sea (AS) and tropical Indian Ocean (TIO). The nucleation mode particles (radius less than 0.1 μm) which are mainly due to the precursor gases from anthropogenic sources carried by the winds influencing the oceanic regions showed a good latitudinal gradient, while the accumulation mode (radius between 0.1 and 1 μm) particles which are longer-lived as compared to the nucleation mode and can be dispersed to long distances showed almost the same percentage contribution over all the regions [*Ramachandran and Jayaraman*, 2002]. Figure 5b represents the model estimates for the time series of species contributions to submicronic dry aerosol mass concentration

for the days of the ship cruise expedition of *Sagar Kanya*. The model estimates dust (two size bins: submicronic and supermicronic), and sea salt (in 10 size bins between 0.045 and 20 μm at 80% relative humidity), but do not have size segregated estimations for the species of sulfate, OM and BC. The submicron mass concentrations are compared from model in relation with that of sum of accumulation and nucleation mode from measurements. In general, the model estimates of total dry surface mass concentration in comparison to measurements corrected to 0% RH are underestimated by a factor of 5 to 10. The model has been extensively evaluated with the INDOEX measurements of *Reddy et al.* [2004]. In the present work, we have used the same version of model with the region tagged emissions to carry out source evaluation of aerosols. Comparison of modeled surface mass concentrations for various species of sulphate, black carbon (BC), organic matter (OM), inorganic matter, and sea salt (please refer to *Reddy et al.* [2004, Figures 2 and 3]) showed that the model captured the north to south gradient in measured concentrations, but over the region of largest concentrations (5 to 10°N), modeled sulphate, BC, and dust concentrations were estimated a factor of 2 to 3 lower than the measured values. The OM and sea salt showed a better agreement with the measurements. It is to be noted that measurements of aerosol surface mass concentration on board *Sagar Kanya* were taken at ambient relative humidity. The correction for the RH factor to the measurements were applied taking into account scaling factors variation with relative humidity as given by *Ramachandran and Jayaraman* [2002, Table 3]. This was done to scale the measurements taken at ambient RH to 0% RH. The scaling factor estimates did not take explicitly the RH growth effects due to individual aerosol component such as sulfate, organic matter. The scaling factors were derived for aerosol size distributions made of water soluble aerosols (*Hess et al.*, 1998) and sea salt (accumulation) and sea salt (coarse) modes. Another factor leading to large discrepancy could be due to the differences in the mode radius of individual aerosol component used in determining the scaling factors [*Hess et al.*, 1998] and the values used in LMD-GCM. We also compare the modeled aerosol optical depth and *Sagar Kanya* measurements which is discussed later in the text.

[12] On evaluating the species composition from model estimates for the days of the ship cruise expedition of *Sagar Kanya*, it is found that sulfate and organic matter contribute mainly to the species composition on days from 20 January (DOY 20) to 30 January (DOY 30) when the ship traverses over coastal India and Arabian Sea and starts to traverse toward the tropical Indian Ocean indicating the transport mainly from the Indian region, based on emission composition analysis presented in Figure 2. Sea salt and sulfate contribute mainly to the species composition from 1 February (DOY 32) to 23 February (DOY 54) when the ship traverses over tropical Indian Ocean, indicating transport mainly from oceanic regions. Contribution from organic matter, sulfate and dust to the total aerosol species composition starts to peak up from 24 February (DOY 55) as the ship traverses near to the Arabian Sea region so that on 25 February (DOY 56), dust along with sulfate and organic matter contribute mainly to species composition, indicating transport from both Indian regions and Africa-west Asia, while that from 26 February (DOY 57) to 28 February (DOY 59), sulfate channel declines, and it is dust followed by organic matter which mainly contributes to the species composition, indicating transport mainly from Africa-west Asia. This is also supported by back trajectory analysis shown in Table 1 and is consistent with *Ramachandran and Jayaraman* [2002, Figure 11a]. From 1 March (DOY 60), organic matter channel declines and sulfate starts to peak up from 2 March (DOY 61) so that aerosol species composition is mainly contributed from both dust and sulfate species, indicating transport mainly from northwest part of India. This is also supported by back trajectory analysis shown in Table 1 and is consistent with *Ramachandran and Jayaraman* [2002, Figure 11b]. From 3 March (DOY 62) to 7 March (DOY 66) dust channel declines and now the aerosol species composition is composed mainly of sulfate species, indicating transport from Indian region. From 8 March (DOY 67) to 11 March (DOY 70), both dust and organic matter again starts to peak up with species composition composed of contributions from both sulfate and dust species mainly on 8 March (DOY 67), while sulfate, dust, and organic matter on 10 March (DOY 69) and 11 March (DOY 70), indicating transport from both Africa-west Asia and Indian region.

[13] Figure 6a shows the aerosol optical depth (AOD) measured on board *Sagar Kanya* at 500 nm and from model estimates (Figure 6b) at 550 nm sampled for the days of the ship cruise expedition of *Sagar Kanya*. The model estimates for AOD agrees relatively well with the *Sagar Kanya* measurements on almost all days except on few days (DOY 24, 60, 65, 66, 67) when the model estimates are underestimated by a factor of 1.5 to 2. This factor of model underestimation falls within the range of 2 to 3 as reported by *Reddy et al.* [2004] on evaluation of model estimates from measurements made from other platforms during INDOEX. The reasons for underestimation of model was attributed to a spurious overestimation of precipitation rate in the model over the Arabian Sea and tropical Indian ocean and inaccuracies in the wind fields of ECMWF which are used to nudge the model, but there is likely to be as well an underestimation of some of the aerosol sources in the model [*Reddy et al.*, 2004]. Though model estimates are underestimated, it is a valuable tool to understand the chemical species composition and the source region evaluation to the aerosol measurements of the *Sagar Kanya*. This is because the pattern of emissions consisting of the regional emission composition of aerosol species as shown in Figure 2 are expected to be correct.

[14] In general, AOD species composition as estimated from model is mainly contributed by sulfate and organic matter on all days except on 10 and 11 March (DOY 69 and 70) when dust also contributes almost equally to that of sulfate and organic matter indicating elevated transport of dust species on these days. A high AOD is estimated when the ship traverses over coastal India followed by that over Arabian Sea and a low value over tropical Indian Ocean. Over CI and AS, species contribution to AOD comprises mainly sulfate species followed by organic matter and black carbon while over TIO, composition mainly comprises contributions from sea salt and sulfate species. This is consistent with measurements from *Sagar Kanya* which showed the presence of more absorbing aerosols over CI and AS as compared to that at TIO with mean values of single scattering albedo of 0.88 (CI), 0.93 (AS), and 0.99 (TIO) [*Ramachandran and Jayaraman*, 2002]. Low values of

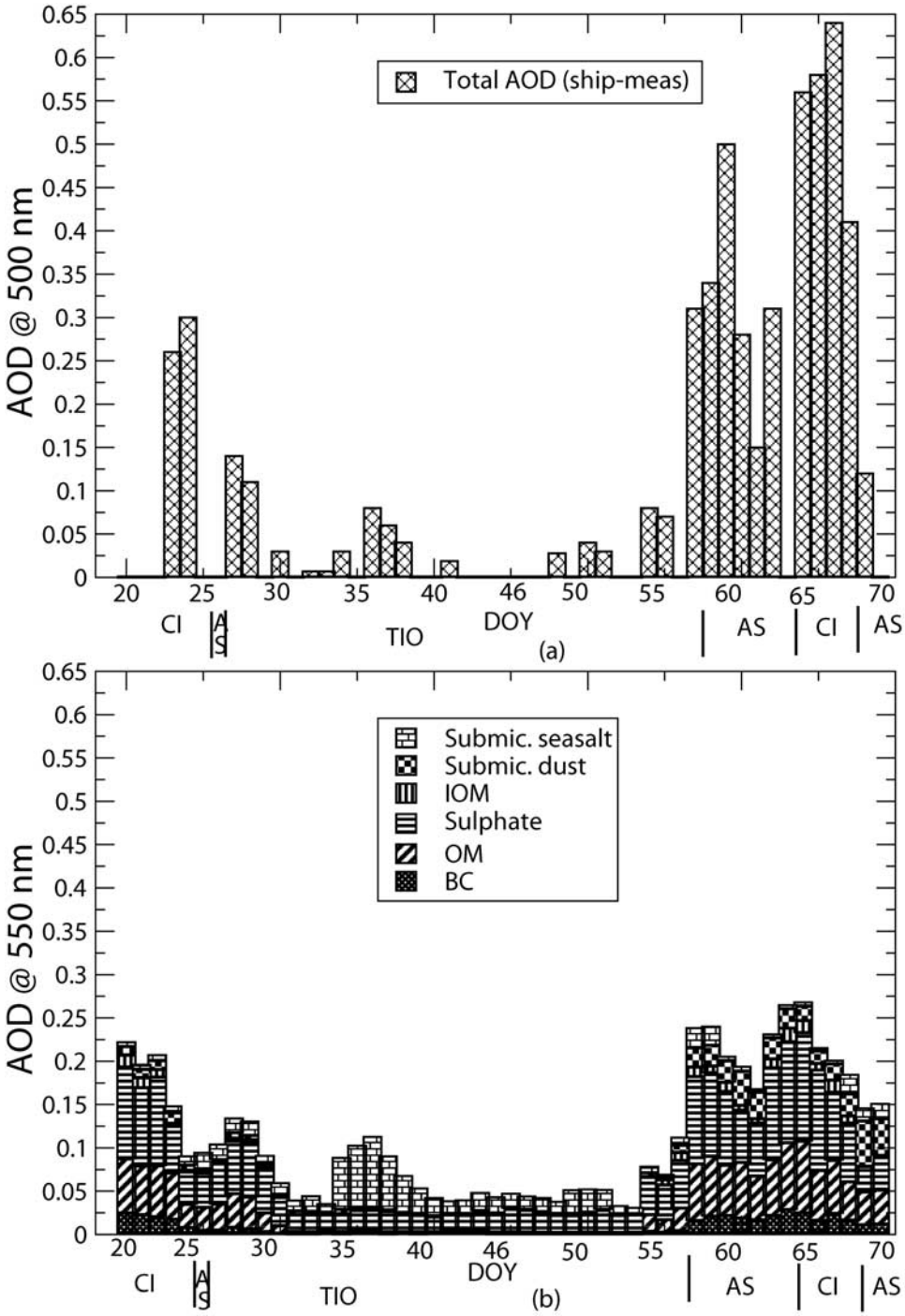

Figure 6. (a) Time series for the aerosol optical depth measured at 500 nm on board *Sagar Kanya* during the INDOEX IFP and (b) species contributions to aerosol optical depth at 550 nm from model estimates for the days of the ship cruise expedition of *Sagar Kanya* during INDOEX-IFP. DOY represents days of the year from 20 January to 11 March 1999. Traverse of the ship over the oceanic regions are represented by CI (coastal India), AS (Arabian Sea), and TIO (tropical Indian Ocean).

single scattering albedo over CI and AS are due to the presence of soot particles emanating from fossil fuel and biomass burning and transported from the continent.

[15] Different features of AOD and that of surface mass concentration are also estimated on some of the days (DOY 20, 59, 69, 70). A high AOD is estimated on 20 January (DOY 20) as compared to that of 22 and 23 January (DOY 22 and 23) though the surface mass concentration showed low value on 20 January (DOY 20) as compared to that on 22 and 23 January (DOY 22 and 23) inferring elevated transport of aerosol species on 20 January (DOY 20). Peaked surface mass concentration on 28 February (DOY 59) is due to an

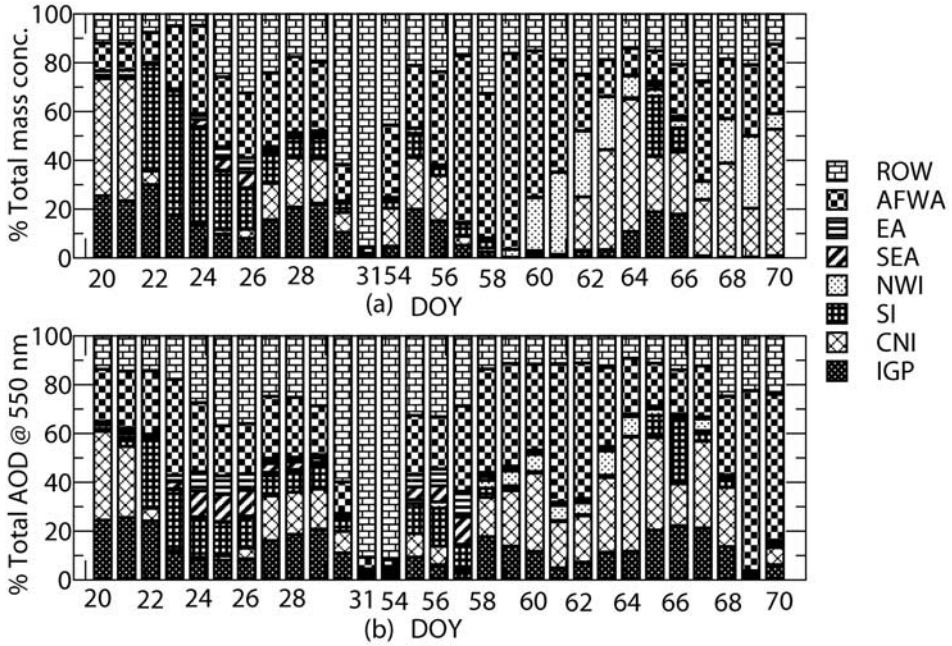

Figure 7. Estimates of aerosol transport from classified source regions from region-tagged simulations for (a) aerosol surface mass concentration and (b) aerosol optical depth averaged for the days of the ship cruise expedition of *Sagar Kanya* during INDOEX-IFP. DOY represents days of the year from 20 January to 11 March 1999.

episodic transport of dust species while AOD shows maximum contributions from organic matter and sulfate species. On 10 March (DOY 69) and 11 March (DOY 70), AOD (largely contributed from dust species) shows a decline though the surface mass concentration (largely contributed from sulfate and organic matter) have high values as compared to previous days indicating the elevated transport of species with low extinction efficiency such as dust species.

[16] Overall, the estimates sampled for the times and locations of *Sagar Kanya* cruise (Figures 5 and 6) captures the latitudinal gradient as reported in INDOEX studies [*Rhoads et al.*, 1997; *Gupta et al.*, 1999; *Moorthy et al.*, 2001] showing the presence of high aerosol surface mass concentration and optical depth when the ship cruises over coastal India and the Arabian Sea as compared to that over the tropical Indian Ocean. Aerosol species is mainly composed of sulfate and organic matter during the early part of its cruise when the ship was mainly influenced by air masses from the Indo-Gangetic plain, central India or south India whereas dust species dominated during its cruise in late February and early March over the Arabian Sea when the ship was influenced by air masses from Africa-west Asia or northwest India. However, a typical clean marine aerosol dominated by sea salt was encountered during February when the ship cruised in the tropical Indian Ocean and was mostly influenced by marine air masses. This corroborates the measurements analysis which showed the presence of heavy pollution including high sulfate, organic matter, black carbon, and inorganic matter in the air masses from Arabia and the Indian subcontinent in addition to the episodic transport of dust from Arabia than that from marine air masses [*Reiner et al.*, 2001; *de Gouw et al.*, 2001; *Gabriel et al.*, 2002; *Mayol-Bracero et al.*, 2002; *Leon et al.*, 2001; *Quinn et al.*, 2002; *Ball et al.*, 2003].

3.3. Identification of Source Regions

[17] Identification of source regions, contributing to both the aerosol surface mass concentration and optical depth, is done through the aerosol transport experiments in the LMD-ZT GCM with region-tagged emissions from the eight source regions defined earlier. The definition of the spatial extent of ROW, results in local sea salt and long-range transported aerosols from regions outside the defined source regions, i.e., northern Asia, north and south America, and Australia, being included in this category. These predictions are evaluated with back trajectory analysis at corresponding ship positions for overlapping time periods, specifically to understand differences in transport pathways at different heights in the atmosphere.

[18] Figure 7 shows the relative contributions of the eight source regions to the submicron aerosol mass concentration averaged between 0 to 500 m heights, corresponding to the surface concentrations measured aboard *Sagar Kanya*, as well as to the AOD, from the aerosol column. The simulation results were sampled at times and various locations during the cruise. Figures 8a–8c and Figures 8d–8f disaggregate the information of Figure 7 for the species of BC, OM and, sulfate. This analysis is presented for the period from 20 January (DOY 20) to 31 January (DOY 31), and from 23 February (DOY 54) to 11 March (DOY 70). From DOY 31 to 54, typical clean marine aerosol dominated by sea salt was encountered. During this period a near uniform aerosol composition, when the ship was in the tropical Indian Ocean, which consisted mostly of sea salt from the local ocean regions and some sulfate (as seen from

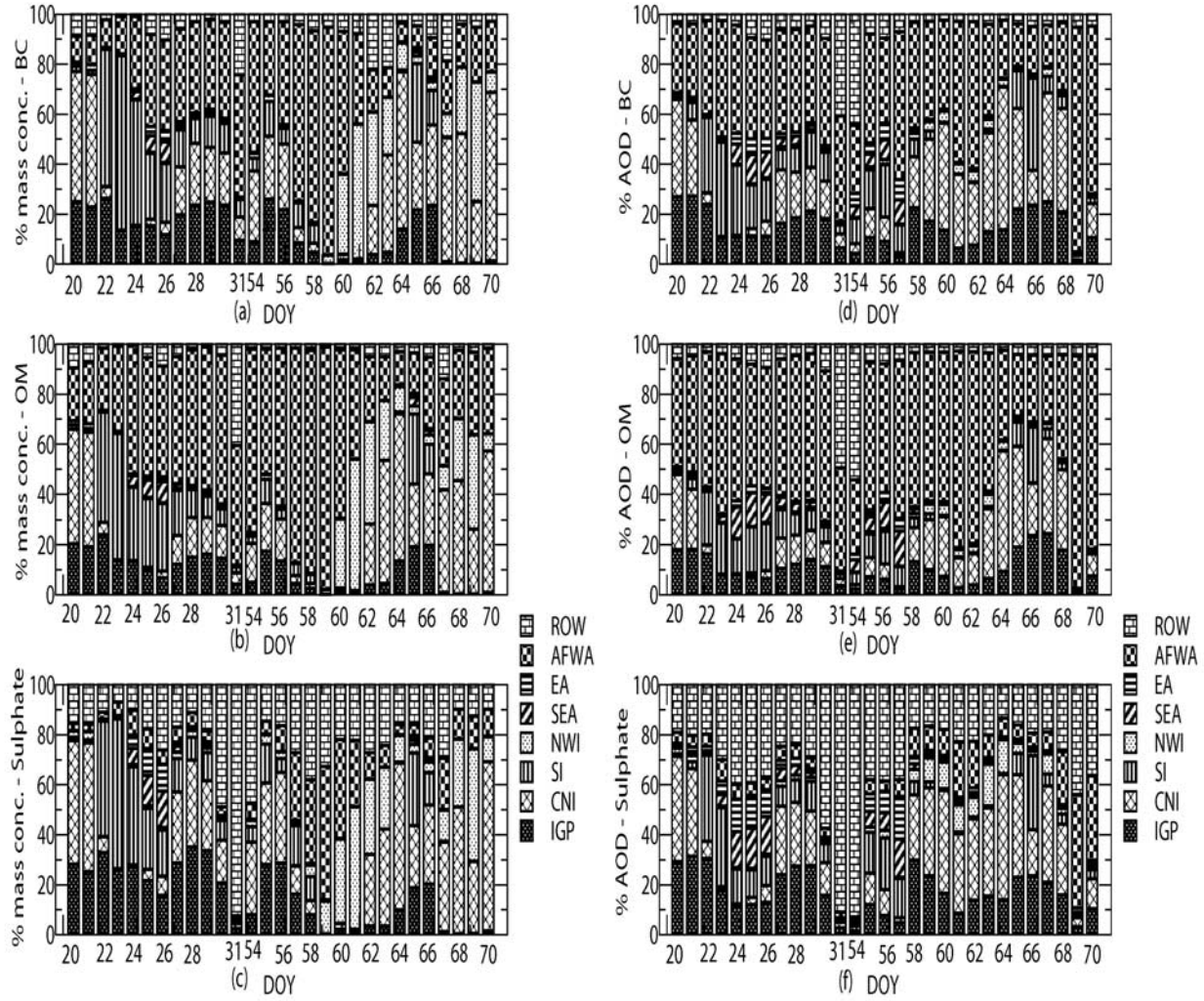

Figure 8. Estimates for aerosol transport from classified source regions from region-tagged simulations for (a–c) aerosol surface mass concentration and (d–f) aerosol optical depth for the aerosol species of BC, OM, and sulfate averaged for the days of the ship cruise expedition of *Sagar Kanya* during INDOEX-IFP. DOY represents days of the year from 20 January to 11 March 1999.

the Figure 5b) transported from the rest of the world (ROW). Also, regional contributions to dust are not shown in Figure 8, as it was mainly contributed from Africa-west Asia (AFWA) with small contributions on some specific days from northwest India (NWI) as discussed later in the text.

[19] Distinct regional contributions to aerosols are seen during the *Sagar Kanya* cruise (Figures 7 and 8). Aerosol emissions from the Indian subcontinent were primarily responsible for surface concentrations during the early part of the cruise (DOY 20–25), when the ship was in the coastal Indian region, and were composed largely of organic matter, sulfate and some fly-ash (Figure 5b). About 50% of the total surface-mass concentration on DOY 20 and 21 is contributed from central India in corroboration with our back trajectory analysis (back trajectories show that air masses spent a long time over central India on these two days) whereas south India contributes almost 20 to 50% to the total surface mass concentration from DOY 22 to 25, with contribution from Indo-Gangetic plain confined between 10 to 30% for the period. The low contribution from the Indo-Gangetic plain as compared to central India and south India may be due to an underestimation of emission flux over the IGP. The refinement in the spatial distribution of emissions from residential biomass energy use and the spatial and temporal distribution of emissions from open burning of forest and agricultural biomass may help in closing some of the discrepancy between model predictions and measurements as discussed in section 3.2.

[20] Surface BC, OM and sulfate were largely from central India during DOY 20–22 and south India during DOY 22–26 (Figure 8). The contribution from Africa-west Asia to the aerosol optical depth (Figure 7) peaks up for 23 January (DOY 23) in agreement with back trajectory transport at higher heights from Africa-west Asia. AOD due to OM and BC (Figure 8) showed a greater contribution from Africa west Asia and implying long-range transport in elevated atmospheric layers of these species into the INDOEX domain. Back trajectories at 10 to 500 m (refer to Table 1 and Figure 4) passed over the Indo-Gangetic

plain/central India/south India, while those at higher heights of 1000 m (on DOY 22 to 25) and 5000 m (on DOY 21 to 22) passed over Africa-west Asia/Indo-Gangetic plain/central India/south India. The model predictions for source region contributions for the aerosol surface mass concentration and optical depth corroborates the back trajectory analysis.

[21] The contributions from rest of the world (ROW) to the total and sulfate aerosol mass concentration start to increase on DOY 25 as the ship crosses the Arabian Sea and approaches the tropical Indian Ocean with contribution from rest of the world rising to 50% for the sulfate (Figure 8) species on DOY 30 and 90% on DOY 31. The back trajectories stay over oceanic regions. The ship continues to traverse cross the TIO for the period from 29 January (DOY 29) to 27 February (DOY 58). Regional contributions are not shown for DOY 32–53 in Figures 7 and 8, as they were largely from the rest of the world. As seen from Figure 5b, for the period from 1 February (DOY 32) to 22 February (DOY 53), the aerosol mass concentration and optical depth are mainly composed of sea salt, from local marine aerosols, and sulfate originating from ROW, i.e., outside the seven other defined regions. Back trajectories at all heights originated over the Indian Ocean regions. Hence the region-tagged model estimates showing the large influence of transport from oceanic regions is consistent with the back trajectory analysis.

[22] A strong regional signal from Africa-west Asia and from central and northwest India dominated during DOY 56–61 and 65–70 (Figure 7). Surface aerosol concentrations were dominated by dust and AOD by organic matter and sulfate (Figures 5b and 6b). Surface concentrations of BC, OM and sulfate showed strong signals of emissions originating in central and northwest India (Figures 8a–8c), consistent with surface flows from the Indian subcontinent. AOD of BC and OM were dominated by emissions originating in Africa-west Asia, indicating elevated transport channels from this region. This is consistent also with *Verma et al.* [2006], who found plumes of organic matter entering the Indian ocean domain (for example during 20–26 March (DOY 79–85), animation 1, showing the evolution of OM concentrations in the work by *Verma et al.* [2006]). On both 4 and 5 March (DOY 63 and 64) an enhanced contribution from central India (45% on DOY 63 and 60% on DOY 64 as compared to 20% on DOY 62) is estimated and both central India and northwest India contribute to the extent of 60 to 70% to the total surface mass concentration with their contributions to BC, OM, and sulfate species as high as 80%. Peak in contributions from northwest India to surface mass concentration and AOD due to dust (figure not shown) are also estimated on 4 and 5 March (DOY 63 and 64), though the largest contributions come from Africa-west Asia due to high emission flux of dust over it. The fractional contribution of a source region also depends upon the emission density over it as for, e.g., large contributions from Africa-west Asia for OM (DOY 24 to 28) as compared to central India or south India and for dust (DOY 63, 64) as compared to northwest India is due to comparatively high emission flux of both OM and dust over Africa-west Asia. This distinct transport at surface and higher layers is consistent with the observed large variability in the mass ratios of chemical species from aircraft and ship [*Clarke et al.*, 2002] in the INDOEX measurements studies and was attributed to different transport pathways in surface and elevated flows.

[23] On DOY 68–70 surface mass concentration showed an enhanced contribution from central India/northwest India, while the aerosol optical depth showed contributions from Africa-west Asia. Back trajectories on all these three days at all heights passes through Africa-west Asia/northwest India. On these days the ship was traversing near to central India. Stronger offshore surface transport from central India and weaker transport from Africa-west Asia, but stronger elevated transport from Africa-west Asia could explain this observation. It is to be noted that *Ramachandran and Jayaraman* [2002] could make two sets of fit between measured and calculated extinction coefficients over the Arabian Sea corresponding to measurements made for days on 28 February (DOY 59), 9 and 10 March (DOY 68 and 69) 1999 and those for 2 March (DOY 61) and 3 March (DOY 63) 1999, respectively, inferring that refractive indices for these two periods can be different. The model predicted surface mass concentration is largely contributed from dust species transported from Africa-west Asia on 28 February (DOY 59) (Figure 5b) as compared to other days (DOY 61, 63, 68, 69) when the chemical composition to surface mass concentration is contributed almost equally from sulfate, dust, and organic matter. The model indicates distinct chemical compositions for the two periods, which explains the reason for the two fits which could be made with the measurements.

[24] Source regions in this study were chosen on the basis of distinct emission flux composition and observed trajectory pathways and are dissimilar in spatial extent and emission flux strength. In general, inaccuracies in the wind fields used both for back trajectory calculations and to nudge GCM simulations, or in model processes, could more strongly affect the estimated influence of source regions with larger spatial extent or emission flux. In this study, proximate source regions, IGP, CNI, NWI, SEA are of similar spatial extent and emission flux, while SI is both small in extent and has a lower flux. The distant source regions EA, AFWA and ROW are similar in spatial extent and emission flux, but are significantly larger than the proximate regions. The ECMWF winds used in this model are believed to have some inaccuracies associated with them [*Reddy et al.*, 2004]. Model underestimation of surface aerosols and AOD at the Kaashidhoo Climate Observatory about 700 km west and south of the Indian subcontinent, especially in March 1999, was attributed in part to inaccuracies in wind fields leading to lower transport of supermicron dust from Arabia into the INDOEX region. Other potential inaccuracies in the wind fields are not well understood. This could affect the estimated regional contributions (Figure 7) with a potential underestimation of the influence of SI and overestimation of the contribution of the larger distant regions. The consistency of the estimated regional influences with the prevailing overall flow patterns, does not point to a significant discrepancy. However, a sensitivity study of region size and emission flux strength to estimated regional contributions would be needed to examine this further. It is to be noted that the two techniques applied in the present study for the source evaluation of aerosols use the different meteorological inputs. We use back trajectory calculations with HYSPLIT using velocity and temperature fields from NCEP data archives (ftp://www.arl.noaa.gov/

pub/archives/fnl) while the GCM is nudged with the ECMWF wind fields. Intercomparison of two reanalyses (NCEP (1948–1998) and ECMWF (1978–1994)) as presented by *Kistler et al.* [1998] indicated that the reanalyses have generally similar degree of agreement. The present analysis with the GCM estimates and back trajectory analysis showed consistent features on source region contributions. We used a combination of methods to verify the aerosol composition contributed from different regions as estimated from GCM (emission inventory information, back trajectory analysis, region-tagged GCM estimates) which are discussed in sections 3.2 and 3.3. Hence we do not see any obvious reason for discrepancy in the present work using the two techniques with different meteorological inputs [NCEP and ECMWF] in source region analysis. However, it is required to carry out a sensitivity study with the meteorological fields other than ECMWF, for, e.g., from NCEP (National Center for Environmental Protection) and NMWRF (National Center for Medium Range Weather Forecasting) to examine the aerosol transport in GCM. We also believe that the refinement in the spatial distribution of emissions from residential biomass energy use and the spatial and temporal distribution of emissions from open burning of forest and agricultural biomass may help in closing some of the discrepancy between model predictions and measurements.

4. Conclusions

[25] A hybrid approach combining chemical transport and back trajectory modeling was used to evaluate the source regions influencing aerosols measured during the INDOEX-IFP aboard *Sagar Kanya*. In the absence of simultaneous aerosol chemical measurements for the ship cruise, these were predicted in a GCM simulation, which showed that sulfate and organic matter are major constituents when the ship track is close to the continental regions and is influenced by air masses from the Indian subcontinent (DOY 20 to 30), along with domination of mineral dust (DOY 57–59), when the ship track is influenced by air masses from Africa-west Asia, while sulfate and sea salt are major constituents when the ship track is remote from the continent (DOY 40 to 53). Back trajectory analysis showed that the ship cruise measurements were largely affected, at lower heights (surface to 500 m) by air mass flow from regions of India and at higher heights (1000 to 5000 m), by flow from Africa-west Asia traversing northwest India or the Indo-Gangetic plain. The distinct transport at surface and higher layers are estimated from region-tagged GCM simulations for, e.g., DOY 56–61 and 65–70, showing strong signals of emissions of black carbon, organic matter, and sulfate originating in central and northwest India, whereas elevated transport channels of black carbon and organic matter from Africa-west Asia. This is consistent with the back trajectory analysis and in corroboration with INDOEX measurement studies which observed different aerosol properties from aircraft and ship attributed to different transport pathways in surface and elevated flows. However, there is a discrepancy between the predicted regional influence from the two approaches on surface concentrations during 9 to 11 March (DOY 68 to 70), potentially because of surface transport from multiple regions, including long-range transport (Africa-west Asia) along with offshore winds (central India or northwest India) bringing aerosols to the receptor location. The fractional contribution of a source region also depends upon the emission density over it as for, e.g., large contributions from Africa-west Asia for OM (DOY 24 to 28) as compared to central India or south India and for dust (DOY 63, 64) as compared to northwest India is due to comparatively high emission flux of both OM and dust over Africa-west Asia.

[26] Model underprediction is likely both from inaccuracies in ECMWF surface wind fields, which do not transport sufficient surface aerosols from the Indian subcontinent over the ocean and in the emissions input to the model. Refinement in the spatial distribution of emissions from residential biomass energy use and the spatial and temporal distribution of emissions from open burning of forest and agricultural biomass may help in closing some of the discrepancy between model predictions and measurements. Source regions in this study were chosen on the basis of distinct emission flux composition and observed trajectory pathways and are dissimilar in spatial extent and emission flux strength. This could affect the estimated regional contributions, with a potential underestimation of the contribution from south India and overestimation of the contribution of the larger, more distant regions. The consistency of the estimated regional influences with the prevailing overall flow patterns, does not point to a significant discrepancy. However, a sensitivity study of region size and emission flux strength to estimated regional contributions would be needed to examine this further.

[27] **Acknowledgments.** Computing resources at Indian Institute of Technology Bombay were supported through a grant from the Indian Ministry for Human Resource Development. A significant part of this work was accomplished through computing time provided by the "Institut du Développement et des Ressources en Informatique Scientifique" (IDRIS) of the CNRS under projects 031167 and 041167. S. Verma acknowledges support from START and the French Embassy in India for her two visits to LOA (France). This study is part of a collaborative project also supported by the Indo-French Centre for the Promotion of Advanced Research (IFCPAR).

References

Ball, W., R. Dickerson, B. Doddridge, J. Stehr, T. Miller, D. Savoie, and T. Carsey (2003), Bulk and size aggregated aerosol composition observed during INDOEX 1999: Overview of meteorology and continental impacts, *J. Geophys. Res.*, *108*(D10), 8001, doi:10.1029/2002JD002467.

Boucher, O., M. Pham, and C. Venkataraman (2002), Simulation of the atmospheric sulphur cycle in the Laboratoire de Météorologie Dynamique general circulation model: Model description, model evaluation and global and European budgets, *Note Sci.*, *23*, Inst. Pierre Simon Laplace, Paris, France.

Clarke, A., et al. (2002), INDOEX aerosol: A comparison and summary of chemical, microphysical, and optical properties observed from land, ship, and aircraft, *J. Geophys. Res.*, *107*(D19), 8033, doi:10.1029/2001JD000572.

de Gouw, J., et al. (2001), Overview of trace gas measurements on board the Citation aircraft during the intensive field phase of INDOEX, *J. Geophys. Res.*, *106*(D22), 28,453–28,467.

de Laat, A., J. de Gouw, J. Lelieveld, and A. Hansel (2001), Model analysis of trace gas measurements and pollution impact during INDOEX, *J. Geophys. Res.*, *106*(D22), 28,469–28,480.

Draxler, R. R., and G. D. Hess (1998), An overview of the HYSPLIT-4 modeling system for trajectories, dispersion and deposition, *Aust. Meteorol. Mag.*, *47*, 295–308.

Franke, K., A. Ansmann, D. Müller, D. Althausen, C. Venkataraman, M. S. Reddy, and R. Scheele (2003), Optical properties of the Indo-Asian haze layer over the tropical Indian Ocean, *J. Geophys. Res.*, *108*(D2), 4059, doi:10.1029/2002JD002473.

Friedlander, S. K. (1973), Chemical element balances and identification of air pollution sources, *Environ. Sci. Technol.*, *7*, 235–240.

Gabriel, R., O. Mayol-Bracero, and M. Andreae (2002), Chemical characterisation of submicron aerosol particles collected over the Indian Ocean, *J. Geophys. Res.*, *107*(D19), 8005, doi:10.1029/2000JD000034.

Gupta, P. K., R. C. Sharma, S. Koul, D. C. Parashar, T. K. Mandal, and A. P. Mitra (1999), Study of trace gas species including greenhouse gases over the Indian Ocean during INDOEX precampaign cruises of 1996, 1997 and 1998 on Sagar Kanya, *Curr. Sci.*, *76*(7), 944–946.

Habib, G., C. Venkataraman, I. Chiapello, S. Ramachandran, O. Boucher, and M. S. Reddy (2006), Seasonal and interannual variability in absorbing aerosols over India derived from TOMS: Relationship to regional meteorology and emissions, *Atmos. Environ.*, *40*, 1909–1921.

Hess, M., P. Koepke, and I. Schult (1998), Optical properties of aerosols and clouds: The software package OPAC, *Bull. Am. Meteorol. Soc.*, *79*, 831–844.

Hopke, P. K. (2003), Recent developments in receptor modeling, *J. Chemometrics*, *17*, 255–265.

Hourdin, F., and J.-P. Issartel (2000), Sub-surface nuclear tests monitoring through the CTBT xenon network, *Geophys. Res. Lett.*, *27*(15), 2245–2248.

Kasibhatla, P., and A. Arellano (2002), Top-down estimate of a large source of atmospheric carbon monoxide associated with fuel combustion in Asia, *Geophys. Res. Lett.*, *29*(19), 1900, doi:10.1029/2002GL015581.

Kistler, R., et al. (1998), The NCEP-NCAR 50-year reanalysis: Monthly means CD-ROM and documentation, *Bull. Am. Meteorol. Soc.*, *82*, 247–268.

Kulkarni, S., Y. Tang, G. R. Carmichael, and L. Pan (2005), Surface elemental composition of aerosols at Beijing (China), Gosan (Korea) and Tango (Japan) during ACE-Asia, *Bull. Indian Aerosol Sci. Technol. Assoc.*, *17*(1–2), 92–93.

Lal, S., D. Chand, L. K. Sahu, S. Venkataramani, G. Brasseur, and M. G. Schultz (2006), High levels of ozone and related gases over the Bay of Bengal during winter and early spring of 2001, *Atmos. Environ.*, *40*, 1633–1644.

Lelieveld, J., et al. (2001), The Indian Ocean Experiment: Widespread air pollution from south and southeast Asia, *Science*, *291*, 1031–1036.

Leon, J.-F., et al. (2001), Large scale advection of continental aerosols during INDOEX, *J. Geophys. Res.*, *106*(D22), 28,427–28,440.

Li, Z.-X. (1999), Ensemble atmospheric GCM simulation of climate interannual variability from 1979 to 1994, *J. Clim.*, *12*, 986–1001.

Mayol-Bracero, O., R. Gabriel, M. Andreae, T. Kirchstetter, T. Novakov, J. Ogren, P. Sheridan, and D. Streets (2002), Carbonaceous aerosols over the Indian Ocean during INDOEX: Chemical characterization, optical properties and probable sources, *J. Geophys. Res.*, *107*(D19), 8030, doi:10.1029/2000JD000039.

Minvielle, F., et al. (2004a), Modeling of the transport of aerosols during INDOEX 19 99 and comparison with experimental data, part 1: Carbonaceous aerosol distribution, *Atmos. Environ.*, *38*(12), 1811–1822.

Minvielle, F., et al. (2004b), Modeling of the transport of aerosols during INDOEX 19 99 and comparison with experimental data, part 2: Continental aerosol and their optical depth, *Atmos. Environ.*, *38*(12), 1823–1837.

Moorthy, K. K., A. Saha, B. Prasad, K. Niranjan, D. Jhurry, and P. S. Pillai (2001), Aerosol optical depths over peninsular India and adjoining oceans during the INDOEX campaign: Spatial, temporal, and spectral characteristics, *J. Geophys. Res.*, *106*(D22), 28,539–28,554.

Quinn, P. K., D. J. Coffman, T. S. Bates, T. L. Miller, J. E. Johnson, E. J. Welton, C. Neusüss, M. Miller, and P. J. Sheridan (2002), Aerosol optical properties during INDOEX 1999: Means, variability, and controlling factors, *J. Geophys. Res.*, *107*(D19), 8020, doi:10.1029/2000JD000037.

Ramachandran, S. (2005), Aerosol radiative forcing over Bay of Bengal and Chennai: Comparison with maritime, continental, and urban aerosol models, *J. Geophys. Res.*, *110*, D21206, doi:10.1029/2005JD005861.

Ramachandran, S., and A. Jayaraman (2002), Premonsoon aerosol mass loadings and size distributions over the Arabian Sea and the tropical Indian Ocean, *J. Geophys. Res.*, *107*(D24), 4738, doi:10.1029/2002JD002386.

Ramanathan, V., et al. (2001), An integrated analysis of the climate forcing and effects of the great Indo-Asian haze, *J. Geophys. Res.*, *106*(D22), 28,371–28,398.

Rao, P. S. (2005), Arabian Sea monsoon experiment: An overview, *Mausam*, *56*(1), 1–6.

Rasch, P. J., W. D. Collins, and B. E. Eaton (2001), Understanding the Indian Ocean Experiment (INDOEX) aerosol distributions with an aerosol assimilation, *J. Geophys. Res.*, *106*(D7), 7337–7355.

Reddy, M. S., and O. Boucher (2004), Global carbonaceous aerosol transport and assessment of radiative effects in the LMDZ GCM, *J. Geophys. Res.*, *109*, D14202, doi:10.1029/2003JD004048.

Reddy, M. S., and C. Venkataraman (2002a), Inventory of aerosol and sulphur dioxide emissions from India: I—Fossil fuels combustion, *Atmos. Environ.*, *36*, 677–697.

Reddy, M. S., and C. Venkataraman (2002b), Inventory of aerosol and sulphur dioxide emissions from India: II—Biomass combustion, *Atmos. Environ.*, *36*, 699–712.

Reddy, M. S., O. Boucher, C. Venkataraman, S. Verma, J.-F. Leon, and M. Pham (2004), GCM estimates of aerosol transport and radiative forcing during INDOEX, *J. Geophys. Res.*, *109*, D16205, doi:10.1029/2004JD004557.

Reiner, T., D. Sprung, C. Jost, R. Gabriel, O. Mayol-Bracero, M. Andreae, T. Campos, and R. Shetter (2001), Chemical characterisation of pollution layers over the tropical Indian Ocean: Signatures of biomass burning emissions, *J. Geophys. Res.*, *106*(D22), 28,497–28,510.

Rhoads, K. P., P. Kelley, R. R. Dickerson, T. P. Carsey, M. Farmer, D. L. Savoie, and J. M. Prospero (1997), Composition of troposhere over the Indian Ocean during the monsoonal transition, *J. Geophys. Res.*, *102*(D15), 18,981–18,995.

Seinfeld, J. H., and S. N. Pandis (Eds.) (1998), *Atmospheric Chemistry and Physics: From Air Pollution to Climate Change*, 1193 pp., John Wiley, New York.

Streets, D. G., et al. (2003), An inventory of gaseous and primary aerosol emissions in Asia, *J. Geophys. Res.*, *108*(D21), 8809, doi:10.1029/2002JD003093.

Verma, S., O. Boucher, C. Venkataraman, M. S. Reddy, D. Müller, P. Chazette, and B. Crouzille (2006), Aerosol lofting from sea breeze during the Indian Ocean Experiment, *J. Geophys. Res.*, *111*, D07208, doi:10.1029/2005JD005953.

Verver, G., D. R. Sikka, J. M. Lobert, G. Stossmeister, and M. Zachariasse (2001), Overview of the meteorological conditions and atmospheric transport processes during INDOEX 1999, *J. Geophys. Res.*, *106*(D22), 28,399–28,414.

Woo, J.-H., et al. (2003), Contribution of biomass and biofuel emissions to trace gas distributions in Asia during the TRACE-P experiment, *J. Geophys. Res.*, *108*(D21), 8812, doi:10.1029/2002JD003200.

O. Boucher, Hadley Centre, Met Office, Fitzroy Road, Exeter EX1 3PB, UK. (olivier.boucher@metoffice.gov.uk)

S. Ramachandran, Space and Atmospheric Sciences Division, Physical Research Laboratory, Ahmedabad 380009, India. (ram@prl.res.in)

C. Venkataraman and S. Verma, Department of Chemical Engineering, Indian Institute of Technology, Bombay, Mumbai 400076, India. (chandra@iitb.ac.in; shubha@iitb.ac.in)